# Ultrabroad-bandwidth multifrequency Raman generation

Mcdonald, GS, New, GHC, Losev, LL, Lutsenko, AP and Shaw, M

| | |
|---|---|
| **Title** | Ultrabroad-bandwidth multifrequency Raman generation |
| **Authors** | Mcdonald, GS, New, GHC, Losev, LL, Lutsenko, AP and Shaw, M |
| **Type** | Article |
| **URL** | This version is available at: http://usir.salford.ac.uk/id/eprint/18347/ |
| **Published Date** | 1994 |

# Ultrabroad-bandwidth multifrequency Raman generation

**G. S. McDonald and G. H. C. New**

*Laser Optics and Spectroscopy Group, The Blackett Laboratory, Imperial College of Science, Technology and Medicine,
Prince Consort Road, London SW7 2BZ, UK*

**L. L. Losev and A. P. Lutsenko**

*P. N. Lebedev Physical Institute, Leninsky Prospekt 53, 117924 Moscow, Russia*

**M. Shaw**

*Rutherford Appleton Laboratory, Chilton, Didcot, Oxfordshire OX11 OQX, UK*

We report on the modeling of transient stimulated rotational Raman scattering in $H_2$ gas. We predict a
multifrequency output, spanning a bandwidth greater than the pump frequency, that may be generated without
any significant delay with respect to the pump pulses. The roles of dispersion and transiency are quantified.

Multiple high Stokes and anti-Stokes orders are frequently observed in stimulated Raman scattering (SRS). Usually, higher orders are generated under phase-matched conditions and thus are at widely differing angles. This results in a multifrequency beam that is not focusable to a single spot. The much more interesting case is that in which higher orders are generated with a phase mismatch but are collinear. Such a beam may have application to laser fusion.[1,2] Recently multiple orders of comparable amplitude spanning a broad bandwidth were generated with both $H_2$ and $N_2$ gas.[3,4] Previously it was thought that long delays arising from the $T_2$ time of the medium would severely limit the usefulness of the generated spectra.[1,2,4] SRS with identical pump and first-Stokes pulse envelopes (symmetric pumping) has not, to our knowledge, been investigated in the transient regime, in which turn-on effects are important. It is precisely in this regime that we predict the generation of more than 40 orders of comparable magnitude during the local rise time of the pump pulse. The central motivation for this research is the optimization of collisional absorption in high-energy laser-target coupling experiments.[1] The benefits of increased bandwidth are multifold and may improve the efficiency of the laser fusion process and significantly increase the number of alternative experimental configurations.[4] Since the underlying mechanisms involved in this work are fundamental, there may be a much wider range of applications.

To model SRS, we expand the total electric field $E$ in terms of constituent plane waves (the pump and Raman sidebands):

$$E(z,t) = \frac{1}{2} \sum_n F_n(z,t) \exp[i(\omega_n t - k_n z)] + \text{c.c.} \quad (1)$$

Each wave has a complex envelope $F_n$ varying in both longitudinal space $z$ and time $t$ and has a carrier frequency given by $\omega_n = \omega_0 + n\omega_R$ ($n = 0, \pm 1, \pm 2, \ldots$),

where $\omega_0$ and $\omega_R$ are the pump frequency and Stokes shift, respectively. For collinear waves the propagation constants $k_n$ are scalar and given by $\mu_n \omega_n / c$, where $\mu_n$ (Ref. 5) is the refractive index at $\omega_n$ and $c$ is the speed of light. To study the essential physics of the multiline generation process, we recast the standard model[6,7] into a dimensionless form by defining the following: $A_n = F_n / F_0(0,0)$, $Z = gI_0(0)z$, $\tau = t/t_p$, and $\gamma_n = \Delta_n / [gI_0(0)]$, where $gI_0(0)$ is the Raman gain coefficient, $I_n(0) = |F_n(0,0)|^2$, $\Delta_n = (\Delta k_n - \Delta k_{n-1}) - (\Delta k_0 - \Delta k_{-1})$, $\Delta k_n = (\mu_n - 1)\omega_n / c$, and $t_p$ is the input pulse width. In any one configuration the set of normalized mistunings $\gamma_n$ are parameterized by $\gamma_1$. With respect to the resonant driving of a single transition the model equations are

$$\frac{\partial A_n}{\partial Z} = \frac{\omega_n}{2\omega_0} \Big[ P^* A_{n+1} \exp(-i\gamma_{n+1}Z) - P A_{n-1} \exp(i\gamma_n Z) \Big], \quad (2)$$

$$\left( \frac{T_2}{t_p} \right) \frac{\partial P}{\partial \tau} = -P + \sum_j A_j A_{j-1}^* \exp(-i\gamma_j Z), \quad (3)$$

where $T_2$ is the dephasing time of the polarization $P$. Previously attention had centered on the injection of a small Stokes seed at an angle to the pump. However, recent analysis and simulation of the steady-state equations[8] investigated the dependency of bandwidth on the initial Stokes wave and predicted that a cw Stokes seed of amplitude equal to the pump would maximize the generated bandwidth. Here we consider symmetric pumping at $Z = 0$, $A_0(\tau) = A_{-1}(\tau) = \exp(-\tau^2)$ and set all other components initially to zero. Collinear symmetric pumping permits maximum spatiotemporal overlap in the term driving the polarization grating; regions without such overlap could also lead to noise amplification.

In this Letter we model rotational SRS in $H_2$ gas, $\omega_R / (2\pi c) = 587$ cm$^{-1}$, pumped by a second harmonic
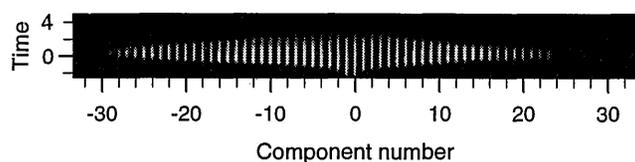
Fig. 1.   Logarithmic plot of light pulses in the generated Raman spectrum. The component number $n$ gives the frequency of each line through $\omega_n = \omega_0 + n\omega_R$. The time scale $\tau$ is in units of the input pulse width $t_p$. Other parameters are $t_p/T_2 = 1$, $Z = 200$, and $\gamma_1 \approx 0.0018$.

of Nd:YAG, $\omega_0/(2\pi c) = 18\,900$ cm$^{-1}$. We solve Eqs. (2) and (3) numerically, using a Runge–Kutta algorithm in $Z$ and a predictor-corrector method in $\tau$. Figure 1 shows the temporal distributions of intensity, $|A_n(\tau)|^2$, of the generated Raman lines for $Z = 200$. Although the logarithmic scale exaggerates pulse widths, the high rate of energy transfer into the higher orders may still be inferred. Closer examination reveals that output spectra are modulated with a rapidly oscillating envelope.[2,8] In the steady-state limit, and neglecting dispersion, we see that this envelope slowly converges to a fixed pattern after $Z = 100$, whereas for finite dispersion the envelope continues to evolve, in both space and time, for $Z$ values as high as several hundred. For transient SRS, time integration of the output pulses yields a clear quantitative picture of the distribution of energy density and also smooths out any temporal modulations. This is shown in Fig. 2, in which $\log_{10} \int_{-\infty}^{\infty} |A_n(\tau)|^2 d\tau$ is plotted. To demonstrate the magnitude of this bandwidth, one may calculate that the visible section of the spectrum spans approximately $18\omega_R$.

Output bandwidth depends on the amplitude of the grating and also on the phase matching of the interacting waves. Figure 3 illustrates the role of dispersion (each data point corresponds to a single simulation). Correlating a number of simulations results in apparently noisy data since small changes at the start of a calculation can lead to large quantitative changes for a fixed $Z$. For each $t_p/T_2$ considered, a large $Z$ is specified to minimize $Z$-dependent variation of the bandwidth. In Fig. 3(a) 10% bandwidths of the time-integrated spectra are shown. This definition of bandwidth reflects the spectral width within which the orders have comparable energy. Choosing $gI_0(0) = 1$ cm$^{-1}$, one can interpret $Z$ as a cell length in centimeters and $\gamma_1$ to be proportional to the gas pressure ($\gamma_1 \approx 0.008$ for 3-atm H$_2$). For $t_p/T_2 \geq 1$ and $\gamma_1 \approx 0$, anti-Stokes orders dominate the output spectrum. Here Stokes orders experience gain suppression,[7,9] while the explicit frequency dependence $\omega_n/\omega_0$ in Eq. (2) enhances the generation of higher frequencies. For increased dispersion the bandwidth reaches a maximum as a result of a rapid increase in the number of the Stokes orders. This peak coincides with an optimal phase mismatch for the parametric interactions, which results in a large number of Stokes and anti-Stokes orders. For large mistunings the parametric interactions are suppressed and generate only weak seeds for the Stokes cascade process. For $t_p/T_2 \ll 1$, dis-

persion also suppresses the generation of Stokes orders, resulting in a relatively monotonic decrease in output bandwidth.

Instantaneous bandwidths (at particular values of $\tau$) may exceed those of time-integrated spectra and can be greater that $50\omega_R$. In Fig. 3(b) the points
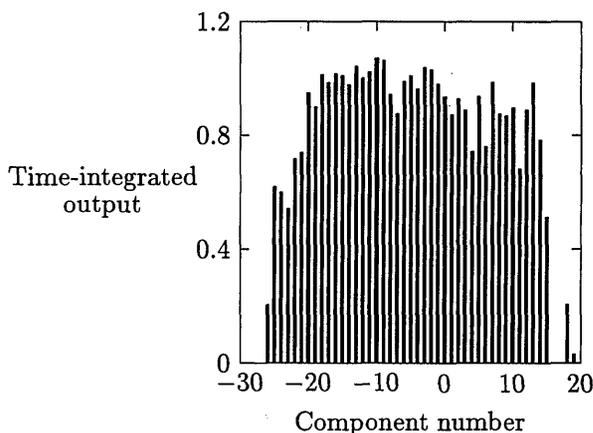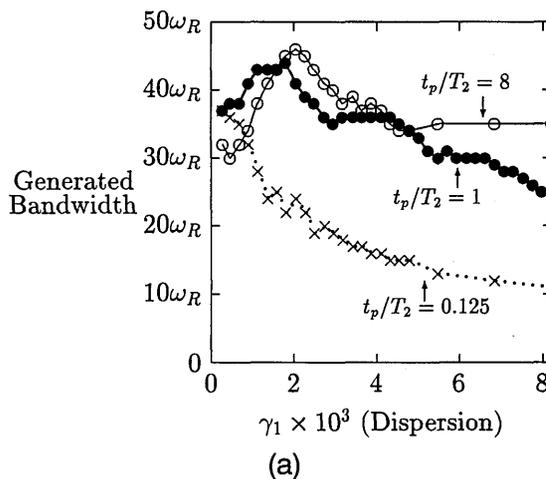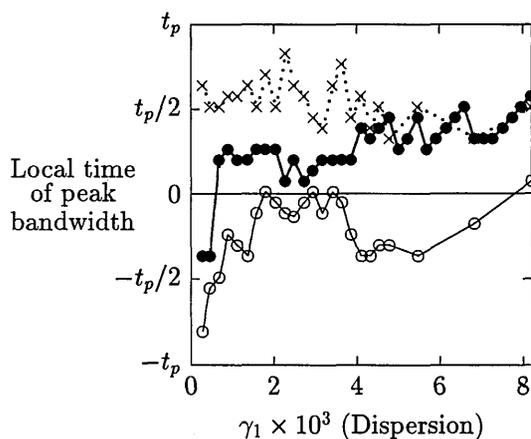


Fig. 2.   Time-integrated intensity of the Raman lines shown in Fig. 1.



(a)



(b)

Fig. 3.   Characteristics of the Raman spectra as a function of dispersion for (a) 10% bandwidths and (b) points in local time for maximum bandwidths [values of $t_p/T_2$ are as indicated in (a)]. $Z = 200$ for $t_p/T_2 \geq 1$ and $Z = 500$ for $t_p/T_2 = 0.125$.
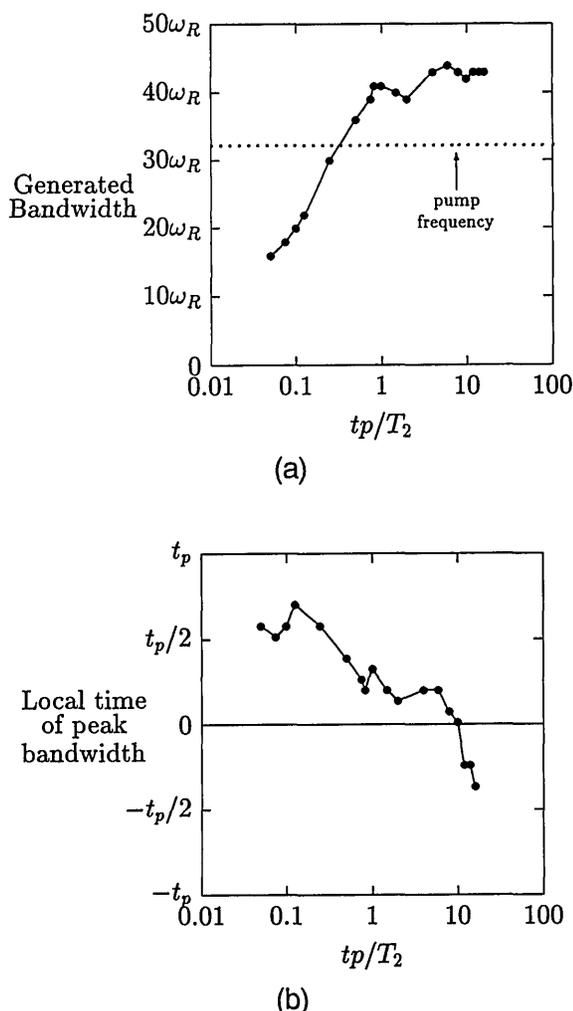
(a)



(b)

Fig. 4. Variation of output characteristics with $t_p/T_2$ for $Z = 500$ and $\gamma_1 \approx 0.0018$: (a) 10% bandwidths and magnitude of the pump frequency in units of the Stokes shift and (b) local times for maximum (instantaneous) bandwidth.

in time for maximim instantaneous bandwidth $\tau_{\max}$ are shown. Bandwidth tends to saturate at large $Z$, whereas $\tau_{\max}$ is local and remains more sensitive to $Z$. We can interpret the overall trends and the level of this sensitivity by correlating these results. Generally, with decreasing $t_p/T_2$, $\tau_{\max}$ is seen to increase. However, the delays shown are still less than the input pulse width $t_p$. For $t_p/T_2 = 0.125$, high dispersion suppresses bandwidth, and consequently $\tau_{\max}$ does not increase greatly. When $T_2 < t_p$, ultrabroad bandwidth may be switched on even during the local rise time of the input pulses.

Figure 4 shows the effect of transiency on bandwidth and $\tau_{\max}$ for a value of $\gamma_1$ that is small but finite. In the direction of the extreme transient limit $(t_p \ll T_2)$ there is a reduction in bandwidth that is due to the simultaneous suppression of Stokes and anti-Stokes orders. Toward the steady-state regime $(t_p \gg T_2)$ bandwidth can be maximal and $\tau_{\max}$ minimal. Even though $t_p/T_2$ varies over 2 orders of

magnitude, symmetric pumping leads to a significant bandwidth that coincides (temporally) with the pump frequency to within a pulse width. It should be stressed that bandwidths of the same order are also predicted for lower $Z$ values. For example, the simulations of Fig. 4 predict a bandwidth of approximately the pump frequency for $t_p/T_2 \geq 1$ and $Z \geq 60$.

In summary, modeling of transient SRS in $H_2$ gas predicts output bandwidths greater than the pump frequency when symmetric pumping is implemented. Previously, long transients were predicted before bandwidths of just several components switch on. We have presented results that suggest that ultrabroad bandwidths may be quickly generated. The experimental realization of just a fraction of the predicted bandwidth would be a significant result. The consideration of additional orders (which are due to a vibrational transition) are not expected to alter our overall conclusions significantly since only the rotational transition is resonantly driven. Furthermore, vibrational orders are more sensitive to dispersion—a sensitivity that is heightened by transient effects. Any vibrational orders that do grow from noise are also expected to form cones that leave the space–time interaction region. Research is in progress to generalize these results through the systematic inclusion of asymmetries and spatiotemporal inhomogeneities[5,10] in the pumping scheme. Studies with more complex models to determine limiting factors that could suppress the generation of such ultrabroad bandwidths need to be undertaken.

## References

1. D. Eimerl, W. L. Kruer, and E. M. Campbell, Comm. Plasma Phys. Controlled Fusion **15**, 85 (1992).
2. D. Eimerl, R. S. Hargrove, and J. A. Paisner, Phys. Rev. Lett. **46**, 651 (1981).
3. M. Hermann, M. Norton, L. Hackel, and D. Twede, in *Conference on Lasers and Electro-Optics*, Vol. 11 of 1993 OSA Technical Digest Series (Optical Society of America, Washington, D.C., 1993), paper ThD2.
4. D. Eimerl, D. Milam, and J. Yu, Phys. Rev. Lett. **70**, 2738 (1993).
5. A. Flusberg, S. Fulghum, H. Lotem, M. Rokni, and M. Tekula, J. Opt. Soc. Am. B **8**, 1851 (1991).
6. A. P. Hickman, J. A. Paisner, and W. K. Bischel, Phys. Rev. A **33**, 1788 (1986).
7. A. P. Hickman and W. K. Bischel, Phys. Rev. A **37**, 2516 (1988).
8. L. L. Losev and A. P. Lutsenko, Kvantovaya Elecktron. (Moscow) **20**, 1054 (1993).
9. Y. R. Shen and N. Bloembergen, Phys. Rev. **137**, A1787 (1965).
10. C. Reiser, T. D. Raymond, and R. B. Mitchie, J. Opt. Soc. Am. B **8**, 562 (1991).